# Equilibrium and Forced Vibration of an Axially Moving Belt with Belt-Pulley Contact Boundaries

**Hu Ding**

*Shanghai Institute of Applied Mathematics and Mechanics, Shanghai University, Shanghai, 200072.*

Axially moving materials have usually dealt with classic boundary conditions, i.e. zero boundaries, such as the simply supported and the fixed ends. In this paper, the dynamics responses of the axially moving belt with belt-pulley contact boundary conditions are studied for the first time. Therefore, due to the fact that non-homogeneous terms are included in the boundary conditions, the traditional generalized eigenvalue method is no longer applicable. In this work, the belt is numerically discretized by using the differential quadrature method (DQM). Iterative schemes are proposed for determining the equilibrium configuration. Harmonic inertia excitation is considered to be the vertical motion of the whole system. The steady-state responses of the forced vibration are also numerically solved by applying the DQM. The parametric effects on the equilibrium configuration and the steady-state response are investigated. The numerical investigations reveal that the radius of the support pulley has significant effects on both the equilibrium configuration and the transition phase of the transverse vibration of the axially moving belt under inertia excitation.

## 1. INTRODUCTION

The objective of this work was to investigate the vibration of an axially moving belt under belt-pulley contact boundary conditions. Axially moving belts are common constituent elements in many engineering systems such as magnetic tapes, textile fibers, and power transmission belts.[1–5] One of the most important problems in these moving belts is the occurrence of large unwanted bending vibrations due to vary excitations, such as the effect of pulley eccentricity, multi-pulse excitation, a time varying velocity and a harmonic axial tension, and external force excitation.[6–10] To ensure that these belts are operating under stable working conditions, it is imperative to understand the vibration characteristics of the moving belts.

Many studies on the free vibration and forced vibration response of axially moving materials can be found in the literature.[11–13] Traditionally, these investigations were focused on the moving materials with classic boundary conditions and either simply supported or fixed ends.[14–16] Wickert obtained the pattern of equilibrium for an axially moving beam with a simply supported end at supercritical transport speed.[17] Seddighi and Eipakchi determined the natural frequency and critical speed of an axially moving beam.[18] Ghayesh, Amabili and Farokhi conducted post-buckling analysis for an axially moving beam undergoing a transverse harmonic excitation.[19] Yao and Zhang carried out the reliability and sensitivity analysis of an axially moving beam with simply supported boundary conditions.[20] Based on a 'cantilever' type boundary conditions, Kelleche, Tatar and Khemmoudj studied the relationship between the dissipation produced by the viscoelastic material and the transversal vibrations caused by the axial motion of the beam.[21] All the research above on the vibration of axially moving systems assumes that the beam was simply supported.

As a result, axially moving materials are considered to be free to bend at the boundary.

By considering the structures with the fixed ends, which were assumed to be unbendable at the border, Oz studied the vibrations of an axially moving beam with variable velocity.[22] Yang and Chen investigated the free non-linear vibration and parametric excitation vibration of axially moving beams.[23,24] Zhang et al. calculated the non-trivial static equilibrium and the steady-state response for moving beams in the supercritical transport speed range under clamped boundary conditions.[25] In order to describe a more general boundary, Chen and Yang proposed hybrid supports.[26] The boundary condition can describe the constraints between the two classical boundary conditions, and can degrade to the simply-supported boundary and the fixed boundary. Based on the hybrid supports, Ding and Chen studied the stability of axially accelerating viscoelastic beams.[27] Yang and Yang presented an exact solution for the supercritical configurations of axially moving beams with fixed boundary conditions.[28] More generally, Park and Chung presented a study on the dynamic analysis of an axially moving beam with intermediate spring supports.[29] Bagdatli and Uslu proposed that axially moving beams have simple and clamped support conditions as a combination of ideal and non-ideal boundaries with a weighting factor.[30] However, all of the above-mentioned studies on axially moving materials were for homogeneous boundary conditions. The study of homogeneous boundary conditions, to a certain extent, can explain the vibration of axially moving material. However, the non-homogeneous boundary conditions that are closer to the pulley-contact actual situation will have an effect on the vibration characteristics of the axially moving belt and are always unknown.

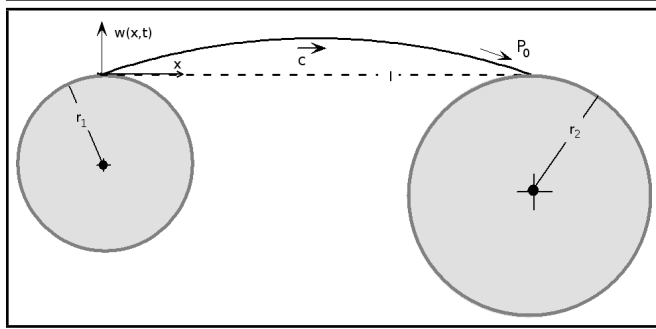In light of the lack of research for the axially moving belts

**Figure 1.** Mechanical model of an axially moving belt with belt-pulley contact boundaries.

under pulley-contact non-homogeneous boundary conditions, the present paper studied the effects of the non-homogeneous boundaries on the free and forced vibrations of the axially moving belt. The differential quadrature method was adopted to numerically solve the equilibrium configuration and the forced vibration responses. The effects of the radius of the support pulley on the static and dynamics of the bending vibrations of the axially moving belts were mainly investigated.

## 2. DYNAMIC MODEL

The Mechanical dynamics model of an axially moving belt with length $l$ and belt-pulley contact boundary conditions is shown in Fig. 1, where the symbols $x$ and $t$ were, respectively, the axial and time coordinates. $r_1$ and $r_2$ were the radius of the left and right support pulleys. $c$ and $P_0$ were the moving speed and the initial static axial tension of the belt and were considered to be constant and uniform, respectively. The whole system was subjected to a vertical harmonic displacement excitation $B\cos(\Omega t)$, where $B$ and $\Omega$ were, respectively, the amplitude and frequency of the excitation.

By only considering the bending vibration of the belt described by the transverse displacement $w(x,t)$, the following governing equation of the transverse vibration of the moving belt was derived by using Newton's second law of motion

$$\rho A(w_{,tt} + 2cw_{,xt} + c^2 w_{,xx}) + M_{,xx}(x,t) - P_0 w_{,xx} = B\rho A\Omega^2 \cos(\Omega t); \quad (1)$$

where $\rho$ and $M$, respectively, represented the density and the bending moment of the belt. $A$ was the cross-sectional area. Moreover, a comma preceding $x$ or $t$ denoted partial differentiation with respect to $x$ or $t$. The material of the viscoelastic belt was assumed to obey the Kelvin constitution relation. The linear moment-curvature relationship was adopted based on the Euler-Bernoulli theory[31]

$$M(x,t) = \left(E + \eta\frac{\partial}{\partial t}\right) I w_{,xx}; \quad (2)$$

where $E$ and $I$ were Young's modulus and the area moment of inertial of the moving belt, $EI$ was used to account for the bending stiffness, respectively. Therefore, the governing equation of the bending vibration of the axially moving belt is de-

rived as[10]

$$\rho A(w_{,tt} + 2cw_{,xt} + c^2 w_{,xx}) - P_0 w_{,xx} + \left(E + \eta\frac{\partial}{\partial t}\right) I w_{,xxxx} = B\rho A\Omega^2 \cos(\Omega t); \quad (3)$$

with the boundary conditions as following[32,33]

$$w(0,t) = 0, w(l,t) = 0, EI w_{,xx}(0,t) = -EI/r_1, EI w_{,xx}(l,t) = -EI/r_2. \quad (4)$$

One can find that there were non-homogeneous boundary conditions. The major goal of this work was to disclose the influence of these non-homogeneous boundary conditions on the vibration characteristics of the axially moving belt. By defining the following dimensionless variables and parameters

$$x \leftrightarrow \frac{x}{l}; \quad (5a)$$

$$w \leftrightarrow \frac{w}{l}; \quad (5b)$$

$$t \leftrightarrow t\sqrt{\frac{P_0}{\rho Al^2}}; \quad (5c)$$

$$c \leftrightarrow c\sqrt{\frac{\rho A}{P_0}}; \quad (5d)$$

$$\alpha = \frac{I\eta}{l^3\sqrt{\rho A P_0}}; \quad (5e)$$

$$k_f = \sqrt{\frac{EI}{P_0 l^2}}; \quad (5f)$$

$$b = \frac{B}{l}; \quad (5g)$$

$$\omega = \Omega\sqrt{\frac{\rho Al^2}{P_0}}; \quad (5h)$$

the dimensionless equation was derived as

$$w_{,tt} + 2cw_{,xt} + (c^2 - 1)w_{,xx} + k_f^2 w_{,xxxx} + \alpha w_{,xxxxt} = b\omega^2 \cos(\omega t); \quad (6)$$

with the dimensionless boundary conditions as following

$$w(0,t) = 0; \quad (7a)$$

$$w(1,t) = 0; \quad (7b)$$

$$w_{,xx}(0,t) = -l/r_1; \quad (7c)$$

$$w_{,xx}(1,t) = -l/r_2; \quad (7d)$$

where the dimensionless parameter, $k_f^2$ denoted the bending stiffness of the moving belt, $\alpha$ accounted for the dynamic viscosity.

## 3. THE EQUILIBRIUM CONFIGURATION

In order to study the effect of the non-homogeneous boundary conditions, the non-trivial equilibrium configuration was determined first. By disregarding all time-related items, the equilibrium configuration $\hat{w}(x)$ of equation (6) satisfied

$$(c^2 - 1)\hat{w}'' + k_f^2 \hat{w}'''' = 0. \tag{8}$$

Correspondingly, the boundary conditions of the equilibrium equation were described as

$$\hat{w}(0) = 0; \tag{9a}$$

$$\hat{w}(1) = 0; \tag{9b}$$

$$\hat{w}''(0) = -l/r_1; \tag{9c}$$

$$\hat{w}''(1) = -l/r_2. \tag{9d}$$

The equilibrium solution was solved by using the differential quadrature method (DQM). The following algebraic equations were obtained by numerical discretization

$$\hat{w}_1 = 0; \tag{10a}$$

$$\sum_{k=1}^{N} A_{2k}^{(2)} \hat{w}_k = -\frac{l}{r_1}; \tag{10b}$$

$$(c^2 - 1)\sum_{k=1}^{N} A_{jk}^{(2)} \hat{w}_k + k_f^2 \sum_{k=1}^{N} A_{jk}^{(4)} \hat{w}_k = 0,$$
$$(j = 3, 4, \ldots, N-2); \tag{10c}$$

$$\sum_{k=1}^{N} A_{(N-1)k}^{(2)} \hat{w}_k = -\frac{l}{r_2}; \tag{10d}$$

$$\hat{w}_N = 0; \tag{10e}$$

where the first-order differential quadrature weighting coefficients were calculated as

$$A_{jk}^{(1)} = \begin{cases} \dfrac{\prod\limits_{m=1,m\neq j}^{N}(x_j - x_m)}{(x_j - x_k)\prod\limits_{m=1,m\neq k}^{N}(x_k - x_m)} & \text{for} \quad k \neq j \\ \sum\limits_{k=1,k\neq j}^{N} \dfrac{1}{x_j - x_k} & \text{for} \quad k = j \end{cases}$$
$$j, k = 1, 2, \ldots, N; \tag{11}$$

where $x_1 - x_N$ were the discrete sampling points. The second and higher order derivatives weighting coefficients were calculated respectively by recurrence relationship

$$A_{jk}^{(2)} = \sum_{m=1}^{N} A_{jm}^{(1)} A_{mk}^{(1)} \quad \text{for} \quad j, k = 1, 2, \ldots, N; \tag{12}$$

and

$$A_{jk}^{(r)} = \sum_{m=1}^{N} A_{jm}^{(1)} A_{mk}^{(r-1)} = \sum_{m=1}^{N} A_{jm}^{(r-1)} A_{mk}^{(1)}$$
$$\text{for} \quad r = 3, 4, \ldots, N \quad \text{and} \quad j, k = 1, 2, \ldots, N. \tag{13}$$

Table 1. Properties of the axially moving belt with contact boundaries.

| Item | Notation | Value |
|---|---|---|
| Length of belt | $l$ | 0.3 m |
| Young's modulus | $E$ | $2 \times 10^8$ N/m$^2$ |
| Width | $b$ | 0.02 m |
| Height | $h$ | 0.01 m |
| Density | $\rho$ | 1200 kg/m$^3$ |
| Static tension | $P_0$ | 400 N |
| Viscous damping | $\alpha$ | $5 \times 10^5$ N s/m$^2$ |
| Radius of left pulley | $r_1$ | 0.03 m |
| Radius of right pulley | $r_2$ | 0.05 m |
| Axial speed | $c$ | 10 m/s |
| Amplitude of excitation | $B$ | 0.0002 m |

For a given set of initial iterative values, the algebraic equations was solved by using the following iterative schemes

$$\hat{w}_1 = 0; \tag{14a}$$

$$\hat{w}_2 = \frac{-\dfrac{1}{r_1} - \sum\limits_{k=1,k\neq 2}^{N} A_{2k}^{(2)} \hat{w}_k}{A_{22}^{(2)}}; \tag{14b}$$

$$\hat{w}_j = \frac{-\left[(c^2-1)\sum\limits_{k=1,k\neq j}^{N} A_{jk}^{(2)} + k_f^2 \sum\limits_{k=1,k\neq j}^{N} A_{jk}^{(4)}\right]\hat{w}_k}{(c^2-1)A_{jj}^{(2)} + k_f^2 A_{jj}^{(4)}},$$
$$(j = 3, 4, \ldots, N-2); \tag{14c}$$

$$\hat{w}_{N-1} = \frac{-\dfrac{l}{r_2} - \sum\limits_{k=1,k\neq N-1}^{N} A_{(N-1)k}^{(2)} \hat{w}_k}{A_{(N-1)(N-1)}^{(2)}}; \tag{14d}$$

$$\hat{w}_N = 0. \tag{14e}$$

The physical and geometrical properties of the example moving belt are listed in Table 1. The initial iterative values were set as

$$\hat{w}_j = 0.0001 \sin(\pi x_j), \quad (j = 1, 2, \ldots, N). \tag{15}$$

In this paper, the number of iterations was always set as 100000. Figure 2 presents the comparison of the equilibrium configurations between different discrete sampling points. Figures 2(a) and 2(b), respectively, show the comparison with the different scale and the same scale. The numerical results in Fig. 2 illustrate that the equilibria calculated with different sampling numbers are completely coincidental. Although Fig. 2(a) shows that the support pulley significantly affects the equilibrium, Fig. 2(b) demonstrates that the displacement of the equilibrium is rather small. However, the degree of bending of the belt could be great in the vicinity of the boundaries.

Figures 3 and 4 respectively present the effects of the radius of the support pulley and axially moving speed on the equilibrium configuration. Figure 3 clearly shows that the equilibrium displacement increases with the decreasing radius of
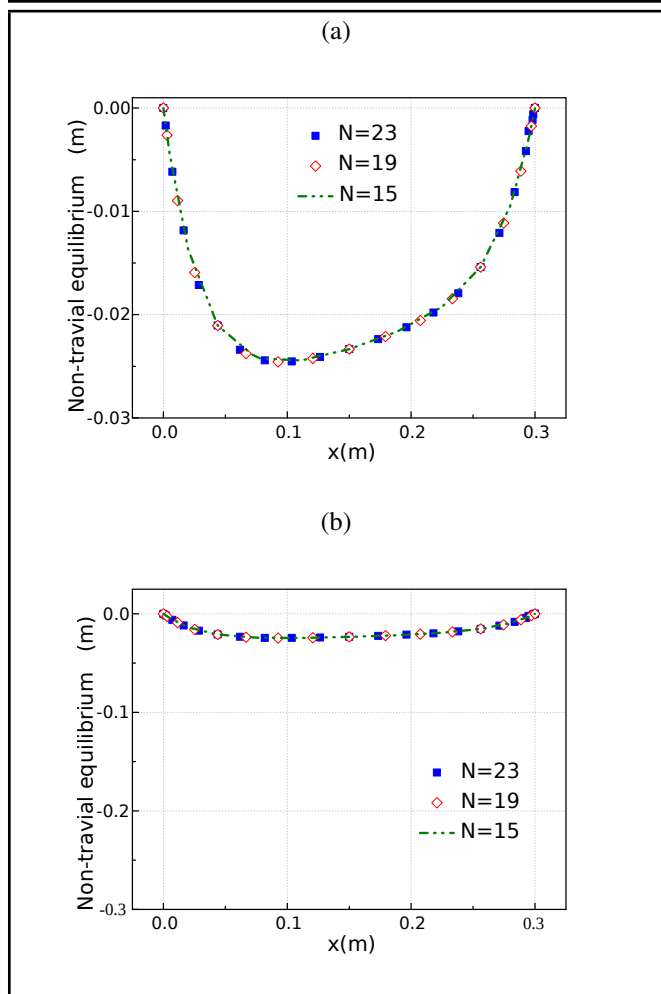
**Figure 2.** Equilibrium configuration of the moving belt with different number of sampling points: (a) with the different scale, (b) with the same scale.
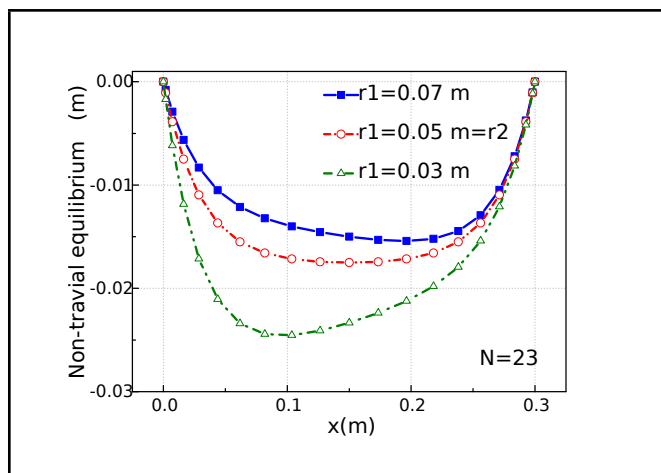


**Figure 3.** Effect of radius of the pulley.

the pulley. It's not hard to understand that, when the radius of the support pulley tends to infinity, the boundary condition of the axially moving belt tends to the classical simple boundary condition. Figure 4 illustrates that the axially moving speed increases the equilibrium displacement. Especially when the moving speed of the belt is large, the impact of the speed on the equilibrium configuration is more sensitive.

The effects of Young's modulus and the initial tension of the
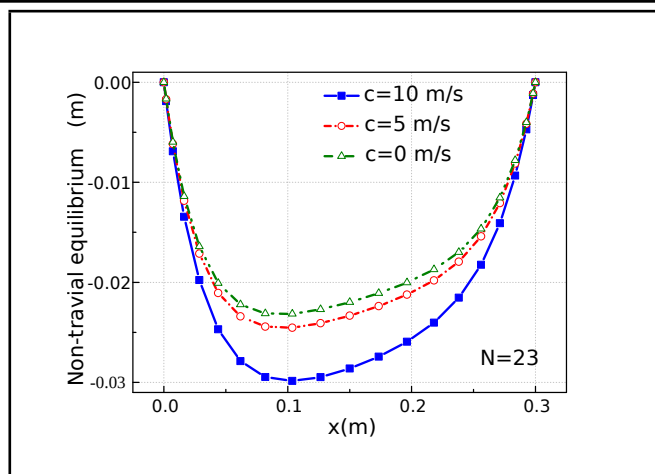


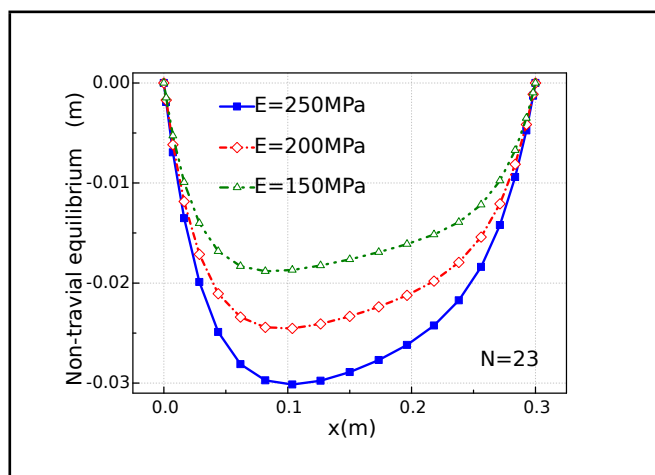**Figure 4.** Effect of the axial moving speed.



**Figure 5.** Effect of the belt stiffness.

moving belt on the equilibrium configuration are described in Figs. 5 and 6, respectively. Interestingly, Fig. 5 demonstrates that the displacement of the equilibrium increases with the increasing belt stiffness. The numerical results in Fig. 6 shows that a strong initial tension can make the static deformation smaller.

## 4. FORCED VIBRATION

The governing partial differential equation of the bending vibration of the axially moving belt with non-homogeneous boundary conditions can be numerical solved. A series of ordinary differential equations can be obtained by using the differential quadrature method (see Eq. (16), on top of the next site).

By discretizing the temporal variables and setting the fixed temporal step as $5 \times 10^{-5}$, $u(x_j, t)$ $(j = 2, 3, \ldots, N - 1)$ was numerically solved using the four-order Runge-Kutta method for given parameter values. Furthermore, the initial values for all numerical examples are set as

$$u(x, 0) = 0; \tag{17a}$$

$$u_{,t}(x, 0) = 0.0001. \tag{17b}$$

$$u(x_1, t) = 0; \tag{16a}$$

$$u(x_2, t) = \left[ -l/r_1 - A_{2(N-1)}^{(2)} u(N-1) - \sum_{k=3}^{N-2} A_{2k}^{(2)} u(x_k, t) \right] / A_{22}^{(2)}; \tag{16b}$$

$$\ddot{u}(x_j, t) + \sum_{k=1}^{N} \left[ 2c A_{jk}^{(1)} + \alpha A_{jk}^{(4)} \right] \dot{u}(x_k, t) - \sum_{k=1}^{N} \left[ (c^2 - 1) A_{jk}^{(2)} + k_f^2 A_{jk}^{(4)} \right] u(x_k, t) = b\omega^2 \cos(\omega t),$$
$$j = 3, 4, \ldots, N-2; \tag{16c}$$

$$u(x_{N-1}, t) = \frac{-l/r_2 - \sum_{k=3}^{N-2} A_{(N-1)k}^{(2)} u(x_k, t) - A_{(N-1)2}^{(2)} \left[ l/r_1 - \sum_{k=3}^{N-2} A_{2k}^{(2)} u(x_k, t) \right] / A_{22}^{(2)}}{A_{(N-1)(N-1)}^{(2)} - A_{(N-1)2}^{(2)} A_{2(N-1)}^{(2)} / A_{22}^{(2)}}; \tag{16d}$$
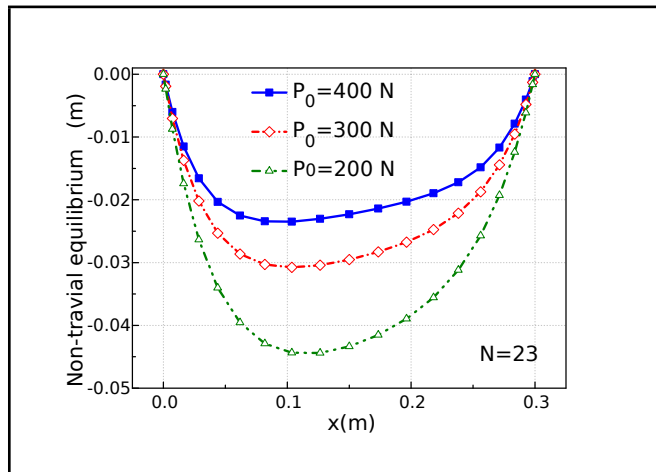
$$u(x_N, t) = 0. \tag{16e}$$



**Figure 6.** Effect of the initial tensionprotect.

For an odd $N$, $u(x_{(N+1)/2}, t)$ was the transverse displacement of the midpoint of the axially moving belt. In the following numerical examples, the number of sampling points $N$ is set as 15.

The time histories of the bending vibration of the midpoint of the axially moving belt were presents in Fig. 7 with the excitation frequency $\Omega = 400$ Hz. In Figure 7(a) and Fig. 7(b), the numerical results describe that a response depending on the initial conditions (19) occurs at the beginning phase, then the transition phase appears, and finally a steady-state response phase forms. Since the axial speed affects the equilibrium configuration and the natural frequencies, Fig. 7(a) shows that the equilibrium position and the steady-state response amplitude of the bending vibration both vary with the axial speed. As shown in Fig. 7(b), the radius of the pulley only changes the equilibrium position. However, the amplitude of the steady-state response does not change with the radius of the support pulley. Nonetheless, the support pulley significantly affects the transition phase of the transverse vibration of the axially moving belt.

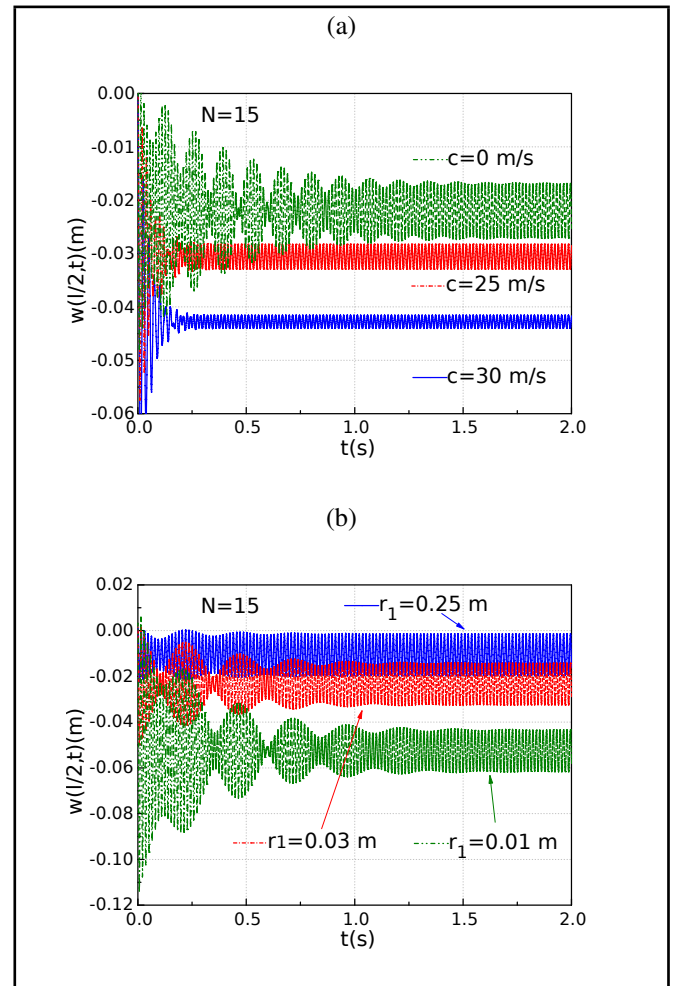In order to determine the stable steady-state response ampli-



**Figure 7.** Time histories of the midpoint of the axially moving belt: (a) with different axial speed, (b) with different radius of the pulley.

tude, the time histories of the axially moving belt were simulated in the time interval of $[0 \text{ s}, 7 \text{ s}]$. For ensuring that transient stage has died away, the time series of the moving belt in the time interval of $[0 \text{ s}, 6.5 \text{ s})$ were discarded. The amplitudes of the steady-state response of the belt were determined by recording the local maximums of $w_{max} = w[(N+1)/2, t]$
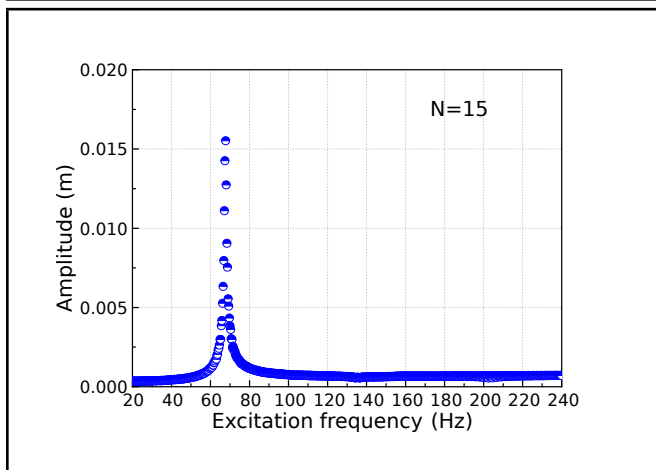
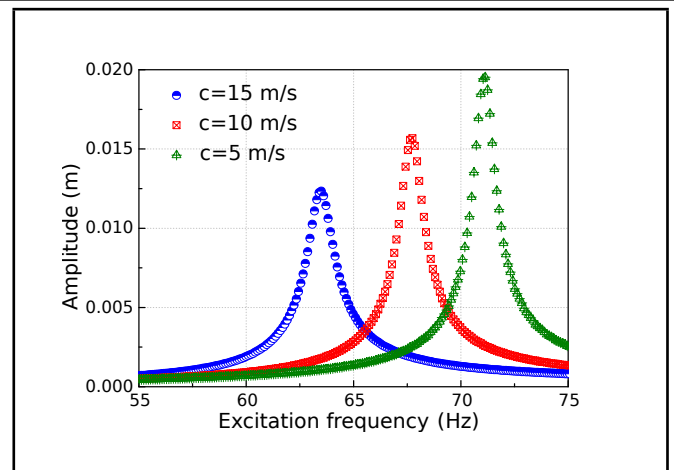**Figure 8.** Steady-state response amplitude.



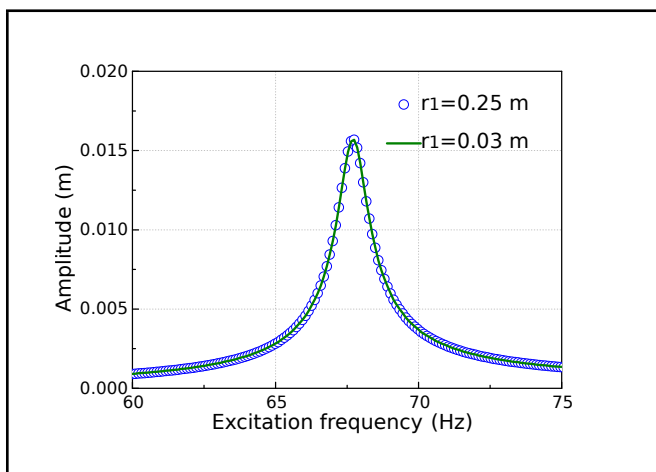**Figure 10.** Effect of the axial speed.



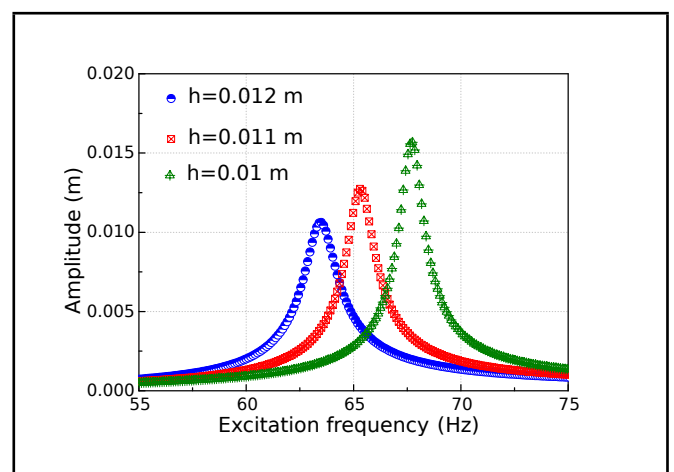**Figure 9.** Effect of the radius of the pulley.



**Figure 11.** Effect of the height of the belt.

in the time interval of [6.5 s, 7 s], as well as the local minimums $w_{min} = w[(N + 1)/2, t]$. Then, the amplitude of the stable steady-state displacement response of the midpoint of the moving belt was obtained by $(w_{max} - w_{min})/2$.

Figure 8 presents the relationship between the response amplitude and the excitation frequency in the frequency interval of [20 s, 240 s]. The numerical results in Fig. 8 clearly show that there is only one resonant peak. In the following numerical examples, only the resonant area was studied. Figure 9 shows that the radius of the support pulley does not affect the steady-state response amplitude, although the equilibrium position changes with the radius.

The effects of the axial speed and the height of the cross section of the belt on the amplitude-frequency relationship are presented in Figs. 10 and 11, respectively. Figures 10 and 11 illustrate that the increase in the axial speed and the height causes the resonant area to move to the low frequency region. However, the resonance intensity is weakened at the same time. In light of this, the larger cross-sectional height corresponds to a smaller resonant frequency. This is different from the static belt. Figures 12 and 13 respectively show the influences of Young's modulus and the initial tension of the axially moving belt on the amplitude-frequency relationship of the transverse bending vibration. As shown in Figs. 12 and 13, the frequency

of resonance and the intensity of resonance both increase as the stiffness and the initial tension of the moving belt increase.

# 5. CONCLUSIONS

For a wide range of belt-pulley coupled dynamic systems, the dynamics of axially moving belts with belt-pulley contact boundary conditions are rarely involved because it is difficult to deal with the non-homogeneous terms. The goal of this work is to study the bending vibration of the axially moving belt with pulley support boundary conditions. The differential quadrature method is applied to discretize the moving belt. Then, the equilibrium configuration caused by the non-homogeneous boundary conditions is numerically solved by proposing an iterative scheme. The forced vibration response is investigated by the DQM. The numerical results show that the equilibrium position and the transition phase of the bending vibration of the moving belt are significantly affected by the support pulleys. Moreover, this work interestingly finds that the larger axial speed or cross-sectional height corresponds to a smaller resonant frequency and a weaker resonant intensity. Furthermore, the larger Young's modulus, or initial tension, draws a stronger resonance intensity.
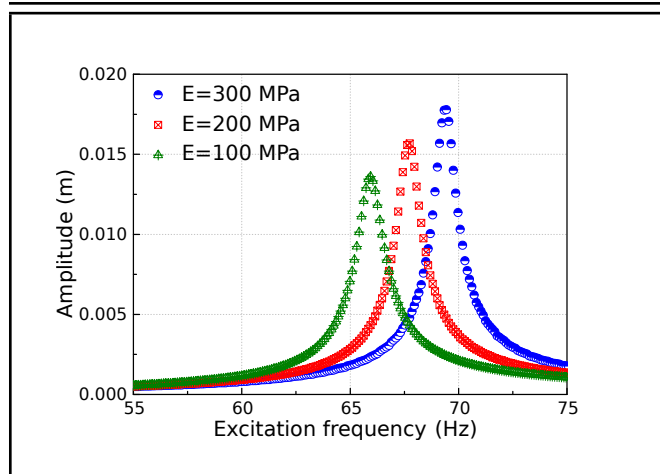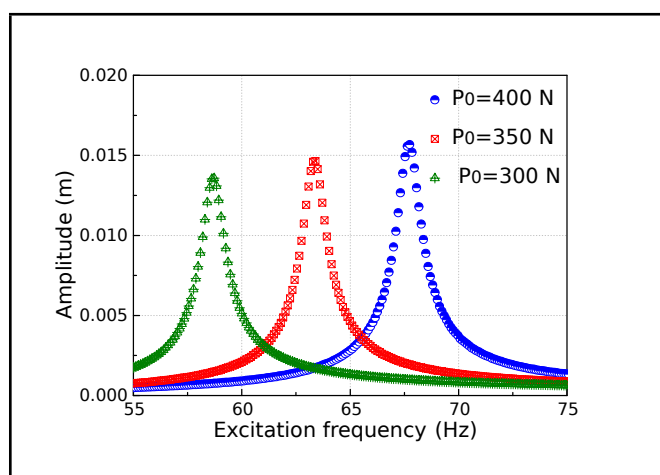
**Figure 12.** Effect of the belt stiffness.



**Figure 13.** Effect of the initial tension.

## ACKNOWLEDGEMENTS

## REFERENCES

[1] Zhang, Y. W., Yuan, B., Fang, B., and Chen, L. Q. Reducing thermal shock-induced vibration of an axially moving beam via a nonlinear energy sink, *Nonlinear Dynamics*, **87** (2), 1159–1167, (2017). https://dx.doi.org/10.1007/s11071-016-3107-4

[2] Wang, Y. Q. and Zu, J. W. Analytical analysis for vibration of longitudinally moving plate submerged in infinite liquid domain, *Applied Mathematics and Mechanics-English Edition*, **38** (5), 625–646, (2017). https://dx.doi.org/10.1007/s10483-017-2192-9

[3] Ding, H., Wang, S., and Zhang, Y. W. Free and forced nonlinear vibration of a transporting belt with pulley support ends, *Nonlinear Dynamics*, **92** (4), 2037–2048, (2018). https://dx.doi.org/10.1007/s11071-018-4179-0

[4] Ding, H., Tan, X., and Dowell, E. H. Natural frequency of a super-critical transporting Timoshenko beam, *European Journal of Mechanics A/Solid*, **66**, 79–93, (2017). https://dx.doi.org/10.1016/j.euromechsol.2017.06.007

[5] Wang, Y. Q., Wan, Y. H., and Zhang, Y. F. Vibrations of longitudinally traveling functionally graded material plates with porosities, *European Journal of Mechanics-A/Solids*, **66**, 55–68, (2017). https://dx.doi.org/10.1016/j.euromechso1.2017.06.006

[6] Pellicano, F., Fregolent, A., Bertuzzi, A., and Vestroni, F. Primary and parametric non-linear resonances of a power transmission belt: Experimental and theoretical analysis, *Journal of Sound and Vibration*, **244** (4), 669–684, (2001). https://dx.doi.org/10.1006/jsvi.2000.3488

[7] Yu, W. Q. and Chen, F. Q. Multi-pulse homoclinic orbits and chaotic dynamics for an axially moving viscoelastic beam, *Archive of Applied Mechanics*, **83** (5), 647–660, (2013). https://dx.doi.org/10.1007/s00419-012-0709-2

[8] Lv, H. W., Li, Y. H., Li, L., and Liu, Q. K. Transverse vibration of viscoelastic sandwich beam with time-dependent axial tension and axially varying moving velocity, *Applied Mathematical Modelling*, **38** (9–10), 2558–2585, (2014). https://dx.doi.org/10.1016/j.apm.2013.10.055

[9] Ozhan, B. B. Vibration and stability analysis of axially moving beams with variable speed and axial force, *International Journal of Structural Stability and Dynamics*, **14** (6), 1450015, (2014). https://dx.doi.org/10.1142/S0219455414500151

[10] Rezaee, M. and Lotfan, S. Non-linear nonlocal vibration and stability analysis of axially moving nanoscale beams with time-dependent velocity, *International Journal of Mechanical Sciences*, **96–97**, 36–46, (2015). https://dx.doi.org/10.1016/j.ijmecsci.2015.03.017

[11] Ding, H., Zhang, G. C., Chen, L. Q., and Yang, S. P. Forced vibrations of supercritically transporting viscoelastic beams, *Journal of Vibration and Acoustics-Transactions of the ASME*, **134** (5), (2012). https://dx.doi.org/10.1115/1.4006184

[12] Marynowski, K. and Kapitaniak, T. Dynamics of axially moving continua, *International Journal of Mechanical Sciences*, **81**, 26–41, (2014). https://dx.doi.org/10.1016/j.ijmecsci.2014.01.017

[13] Ding, H., Huang, L. L., Mao, X. Y., and Chen, L. Q. Primary resonance of traveling viscoelastic beam under internal resonance, *Applied Mathematics and Mechanics-English Edition*, **38** (1), 1–14, (2017). https://dx.doi.org/10.1007/s10483-016-2152-6

[14] Ding, H., Lim, C. W., and Chen, L. Q. Nonlinear vibration of a traveling belt with non-homogeneous boundaries,

*Journal of Sound and Vibration*, **424** (23), 78–93, (2018). https://dx.doi.org/10.1016/j.jsv.2018.03.010

[15] Huang, J. L., Su, R. K. L., Li, W. H., and Chen, S. H. Stability and bifurcation of an axially moving beam tuned to three-to-one internal resonances, *Journal of Sound and Vibration*, **330** (3), 471–485, (2011). https://dx.doi.org/10.1016/j.jsv.2010.04.037

[16] Banerjee, J. R. and Gunawardana, W. D. Dynamic stiffness matrix development and free vibration analysis of a moving beam, *Journal of Sound and Vibration*, **303** (1–2), 135–143, (2007). https://dx.doi.org/10.1016/j.jsv.2006.12.020

[17] Jeronen, J., Saksa, T. and Tuovinen, T. Stability of a tensioned axially moving plate subjected to cross-direction potential flow, *Mathematical Modeling and Optimization of Complex Structures*, **40**, 105–116, (2016). https://dx.doi.org/10.1007/978-3-319-23564-6_7

[18] Wickert, J. A. Nonlinear vibration of a traveling tensioned beam, *International Journal of Non-Linear Mechanics*, **27** (3), 503–517, (1992). https://dx.doi.org/10.1016/0020-7462(92)90016-Z

[19] Seddighi, H. and Eipakchi, H. Natural frequency and critical speed determination of an axially moving viscoelastic beam, *Mechanics of Time-Dependent Materials*, **17** (4), 529–541, (2013). https://dx.doi.org/10.1007/s11043-012-9201-1

[20] Ghayesh, M. H., Amabili, M., and Farokhi, H. Global dynamics of an axially moving buckled beam, *Journal of Vibration and Control*, **21** (1), 195–208, (2015). https://dx.doi.org/10.1177/1077546313486282

[21] Yao, G. and Zhang, Y. M. Reliability and sensitivity analysis of an axially moving beam, *Meccanica*, **51** (3), 491–499, (2016). https://dx.doi.org/10.1007/s11012-015-0232-y

[22] Kelleche, A., Tatar, N. E., and Khemmoudj, A. Stability of an axially moving viscoelastic beam, *Journal of Dynamical and Control Systems*, **23** (2), 283–299, (2017). https://dx.doi.org/10.1007/s10883-016-9317-8

[23] Oz, H. R. On the vibrations of an axially travelling beam on fixed supports with variable velocity, *Journal of Sound and Vibration*, **239** (3), 556–564, (2001). https://dx.doi.org/10.1006/jsvi.2000.3077

[24] Yang, X. D. and Chen, L. Q. Free non-linear vibration of axially moving beams with fixed ends, *Acta Mechanica Solida Sinica*, **18** (3), 242–247, (2005). https://dx.doi.org/10.1007/s10338-005-0530-3

[25] Yang, X. D. and Chen, L. Q. Dynamic stability of an axially accelerating viscoelastic beam with two fixed supports, *International Journal of Structural Stability and Dynamics*, **6** (1), 31–42, (2006). https://dx.doi.org/10.1142/S0219455406001812

[26] Zhang, G. C., Ding, H., Chen, L. Q., and Yang, S. P. Supercritical forced response of coupled motion of a nonlinear transporting beam, *Nonlinear Dynamics*, **70** (4), 2407–2420, (2012). https://dx.doi.org/10.1007/s11071-012-0629-2

[27] Chen, L. Q. and Yang, X. D. Vibration and stability of an axially moving viscoelastic beam with hybrid supports, *European Journal of Mechanics a-Solids*, **25** (6), 996–1008, (2006). https://dx.doi.org/10.1016/j.euromechsol.2005.11.010

[28] Ding, H. and Chen, L. Q. Stability of axially accelerating viscoelastic beams: multi-scale analysis with numerical confirmations, *European Journal of Mechanics a-Solids*, **27** (6), 1108–1120, (2008). https://dx.doi.org/10.1016/j.euromechsol.2007.11.014

[29] Yang, T. Z. and Yang, X. D. Exact solution of supercritical axially moving beams: symmetric and anti-symmetric configurations, *Archive of Applied Mechanics*, **83** (6), 899–906, (2013). https://dx.doi.org/10.1007/s00419-012-0725-2

[30] Park, S. and Chung, J. T. Dynamic analysis of an axially moving finite-length beam with intermediate spring supports, *Journal of Sound and Vibration*, **333** (24), 6742–6759, (2014). https://dx.doi.org/10.1016/j.jsv.2014.07.031

[31] Bagdatli, S. M. and Uslu, B. Free vibration analysis of axially moving beam under non-ideal conditions, *Structural Engineering and Mechanics*, **54** (3), 597–605, (2015). https://dx.doi.org/10.12989/sem.2015.54.3.597

[32] Ding, H., Ji, J.C. and Chen, L.Q. Nonlinear vibration isolation for fluid-conveying pipes using quasi-zero stiffness characteristics, *Mechanical Systems and Signal Processing*, **121**, 675–688, (2019). https://dx.doi.org/10.1016/j.ymssp.2018.11.057

[33] Ding, H. and Zu, J. W. Steady-state responses of pulley-belt systems with a one-way clutch and belt bending stiffness, *Journal of Vibration and Acoustics-Transactions of the ASME*, **136** (4), 041006, (2014). https://dx.doi.org/10.1115/1.4027456

[34] Ding, H., Dowell, E. H., and Chen, LQ. Transmissibility of bending vibration of an elastic beam, *Journal of Vibration and Acoustics-Transactions of the ASME*, **140** (3), 031007, (2018). https://dx.doi.org/10.1115/1.4038733 Ding, H., Lu, Z.Q. and Chen. L.Q. Nonlinear isolation of transverse vibration of pre-pressure beams, *Journal of Sound and Vibration*, **442**, 738–751, (2019). https://dx.doi.org/10.1016/j.jsv.2018.11.028